An Inner-Product Calculus for Periodic Functions and Curves

Anaïs Badoual, Daniel Schmitter, and Michael Unser

***Abstract*—Our motivation is the design of efficient algorithms to process closed curves represented by basis functions or wavelets. To that end, we introduce an inner-product calculus to evaluate correlations and L_2 distances between such curves. In particular, we present formulas for the direct and exact evaluation of correlation matrices in the case of closed (i.e., periodic) parametric curves and periodic signals. We give simplifications for practical cases that involve B-splines. To illustrate this approach, we also propose a least-squares approximation scheme that is able to resample curves while minimizing aliasing artifacts. Another application is the exact calculation of the enclosed area.**

***Index Terms*—Area, basis functions, compact support, correlation, inner product, splines.**

I. Introduction

IT IS common in signal processing to represent continuous-domain signals using basis functions. This approach is prevalent in classical (Shannon-) sampling theory [1]–[3], approximation theory [4], [5], and wavelet theory [6]–[9]. It is also at the heart of (generalized) interpolation [10]. It is characterized by a signal f being represented by a weighted sum of integer-shifted basis functions as

$$f(t) = \sum_{k\in\mathbb{Z}} c[k]\varphi\left(\frac{t}{T} - k\right) \tag{1}$$

where T is the sampling step and $\{c[k]\}_{k\in\mathbb{Z}}$ a sequence of weights that depend on, but are not necessarily equal to, the samples of f. Here, φ is a (real-valued) *generator* such as the sinc function or a B-spline [11]. For practical reasons, φ is often chosen to be of compact support. In classical signal processing, f is required to be square integrable in Lebesgue's sense, which implies that f lives in the Hilbert space $L_2(\mathbb{R})$. The basis $\{\varphi(\frac{\cdot}{T} - k)\}_{k\in\mathbb{Z}}$ generated by the integer shifts of the generator is L_2 stable if it defines a *Riesz basis*: there must exist two positive constants $0 < A, B < \infty$ such that, for all $c \in \ell_2$,

$$A\|c\|_{\ell_2}^2 \leq \frac{1}{T}\left\|\sum_{k\in\mathbb{Z}} c[k]\varphi\left(\frac{\cdot}{T} - k\right)\right\|_{L_2}^2 \leq B\|c\|_{\ell_2}^2.$$

The second fundamental requirement when using the type of expansion given by (1) is that a rescaled version of the model ought to be able to approximate any function as closely as desired as the sampling step T tends to zero. This is equivalent to the *partition-of-unity* condition [11]

$$\sum_{k\in\mathbb{Z}} \varphi\left(\frac{t}{T} - k\right) = 1, \quad \forall t \in \mathbb{R}. \tag{2}$$

A. Periodic Signals and Closed Parametric Curves

For periodic signals, computations can usually be simplified by focusing on a single period [12]–[14]. Without loss of generality, the period can always be normalized to one, and hence, we only consider $t \in [0, 1]$. The representation of f by (1) implies that, if the signal is one-periodic, the sequence c is of period M such as $T = \frac{1}{M}$, where M is a positive integer. In this case, (1) is expressed in terms of the normalized and M-periodized basis functions φ_{per} as

$$\begin{aligned} f(t) &= \sum_{k=0}^{M-1}\sum_{n=-\infty}^{+\infty} c[k+Mn]\varphi(Mt - Mn - k) \\ &= \sum_{k=0}^{M-1} c[k] \underbrace{\sum_{n=-\infty}^{+\infty} \varphi(Mt - Mn - k)}_{\varphi_{\mathrm{per}}(Mt-k)} \end{aligned} \tag{3}$$

where $t \in [0, 1]$. Equation (3) can also be used to represent one-periodic (i.e., closed) parametric curves in 2-D as

$$\boldsymbol{r}(t) = \begin{pmatrix} f_x(t) \\ f_y(t) \end{pmatrix} = \sum_{k=0}^{M-1} \boldsymbol{c}[k]\varphi_{\mathrm{per}}(Mt - k) \tag{4}$$

where the $\{\boldsymbol{c}[k] = (c_x[k], c_y[k])\}_{k\in\mathbb{Z}}$ are now called the *control points* of the curve. An important consideration for selecting the basis functions in (4) is that the parametric form of the model must be preserved through rigid-body transformations. This is guaranteed if the model (4) is *affine invariant*, which means that

$$\mathbf{T}\,\boldsymbol{r}(t) + \boldsymbol{b} = \sum_{k=0}^{M-1} (\mathbf{T}\,\boldsymbol{c}[k] + \boldsymbol{b})\,\varphi_{\mathrm{per}}(Mt - k) \tag{5}$$

where $\mathbf{T}$ is a (2×2) matrix and $\boldsymbol{b}$ is a 2-D vector. The constraint (5) is equivalent to the partition-of-unity condition (2) in [15].

Parametric curves that are represented by compactly supported basis functions are often used to construct active-contour models [16], [17] and to segment bioimages [18]–[20]. More generally, the control-point-based nature of (4) makes this model particularly convenient in applications where user interaction is required [21], [22]. The reason is that the simple adjustment of one control point is enough to adjust the curve locally.

Manuscript received December 19, 2015; revised April 10, 2016; accepted April 13, 2016. Date of publication April 15, 2016; date of current version May 12, 2016. This work was supported by the Swiss National Science Foundation under Grant 200020-162343. The associate editor coordinating the review of this manuscript and approving it for publication was Prof. Marco Lops.

The authors are with the Biomedical Imaging Group, École Polytechnique Fédérale de Lausanne (EPFL), 1015 Lausanne, Switzerland (e-mail: anais.badoual@epfl.ch; daniel.schmitter@epfl.ch; michael.unser@epfl.ch).

Color versions of one or more of the figures in this letter are available online at http://ieeexplore.ieee.org.

Digital Object Identifier 10.1109/LSP.2016.2555139

Definition: To each curve $\boldsymbol{r}_i$ is assigned the couple (φ_i, M_i), where φ_i is the basis function and M_i is the associated number of control points. We express the corresponding M_i-periodized basis function by $\varphi_{i,\mathrm{per}}(t) = \sum_{n\in\mathbb{Z}} \varphi_i(t - nM_i)$. We define the vector $\boldsymbol{\varphi}_i$, of size M_i, that contains the basis $\{\varphi_{i,\mathrm{per}}(M_i \cdot - k)\}_{k\in\mathbb{Z}}$, as

$$\boldsymbol{\varphi}_i(t) = \begin{pmatrix} \varphi_{i,\mathrm{per}}(M_i t) \\ \vdots \\ \varphi_{i,\mathrm{per}}(M_i t - M_i + 1) \end{pmatrix}.$$

The condensed notation

$$\boldsymbol{r}_i(t) = \mathbf{C}_i^{\mathsf{T}} \boldsymbol{\varphi}_i(t) \tag{6}$$

is equivalent to (4). There, $\mathbf{C}_i$ is the $(M_i \times 2)$ matrix defined as

$$\mathbf{C}_i = \begin{pmatrix} c_{x_i}[0] & c_{y_i}[0] \\ \vdots & \vdots \\ c_{x_i}[M_i - 1] & c_{y_i}[M_i - 1] \end{pmatrix}. \tag{7}$$

In the case of 1-D signals, the matrix $\mathbf{C}_i$ collapses to a vector.

B. Inner Products

The exact computation of inner products is a frequent operation in signal and image processing such as for the evaluation of L_2 distances, orthogonal projections, or similarity measurements. Thus, our interest here is in the efficient calculation of the L_2 distance between two curves that may be parameterized with a different number of control points [23], [24]. We express the L_2 inner product between the two closed curves $\boldsymbol{r}_1, \boldsymbol{r}_2 \in L_2([0,1])$ as

$$\begin{aligned} \langle \boldsymbol{r}_1, \boldsymbol{r}_2 \rangle_{L_2([0,1])} &= \int_0^1 \boldsymbol{r}_1^{\mathsf{T}}(t) \boldsymbol{r}_2(t) \mathrm{d}t \\ &= \mathrm{tr}\left(\mathbf{C}_1^{\mathsf{T}} \left(\underbrace{\int_0^1 \boldsymbol{\varphi}_1(t) \otimes \boldsymbol{\varphi}_2(t) \mathrm{d}t}_{\mathbf{A}_{12}} \right) \mathbf{C}_2 \right) \end{aligned} \tag{8}$$

where $\mathbf{A}_{12}$ is the *correlation matrix* of size $(M_1 \times M_2)$ specified as $[\mathbf{A}_{12}]_{k,l} = \langle [\boldsymbol{\varphi}_1]_k, [\boldsymbol{\varphi}_2]_l \rangle_{L_2([0,1])}$ and $\otimes$ denotes the tensor product. To evaluate (8), the entries of the correlation matrix require the evaluation of some integrals. We present in Section II a calculus that facilitates these computations in the continuous domain.

II. Inner-Product Calculus

A. General Calculation

We start by providing a general formula for precomputing the matrix $\mathbf{A}_{12}$ and then discuss a number of situations that can be resolved analytically.

Proposition 1: Let φ_1 and φ_2 be two compactly supported generators with $\mathrm{supp}\{\varphi_1\} = [a_1, b_1]$, $\mathrm{supp}\{\varphi_2\} = [a_2, b_2]$, $M_1 \geq \mathrm{supp}\{\varphi_1\}$, and $M_2 \geq \mathrm{supp}\{\varphi_2\}$. The entries of the $(M_1 \times M_2)$ cross-correlation matrix $\mathbf{A}_{12} = \int_0^1 \boldsymbol{\varphi}_1(t) \otimes \boldsymbol{\varphi}_2(t) \mathrm{d}t$ are given by

$$[\mathbf{A}_{12}]_{k,l} = \frac{1}{M_1} \sum_{m=m_1}^{m_2} a_{12}(-\tau_{k,l,m})$$

where

$$\begin{aligned} a_{12}(t) &= \int_{\mathbb{R}} \varphi_1(u) \varphi_2\left(\frac{M_2}{M_1}(u - t)\right) \mathrm{d}u \\ &= \left(\varphi_1 * \varphi_2\left(-\frac{M_2}{M_1}\cdot\right)\right)(t), \end{aligned}$$

$\tau_{k,l,m} = M_1(m + \frac{k}{M_1} - \frac{l}{M_2})$, $m_1 = \lceil \min(p_1, p_2)) \rceil$, $m_2 = \lfloor \max(1 + p_1, 1 + p_2) \rfloor$, $p_1 = (\frac{1}{M_2}(a_2 + l) - \frac{1}{M_1}(a_1 + k))$, and $p_2 = (\frac{1}{M_2}(a_2 + l) - \frac{1}{M_1}(b_1 + k))$. There, $\lfloor \cdot \rfloor$ and $\lceil \cdot \rceil$ denote the floor and the ceil function, respectively.

The proof of Proposition 1 is given in Appendix A. In the case where the generators are even or odd functions with respect to the same axis, Proposition 1 is simplified as specified by Corollary 1.

Corollary 1: Let φ_1 and φ_2 be two even or odd functions with respect to the same axis of symmetry.

a) The correlation between the one-periodic functions $[\boldsymbol{\varphi}_1]_k$ and $[\boldsymbol{\varphi}_2]_l$ is

$$\begin{aligned} [\mathbf{A}_{12}]_{k,l} = \frac{1}{M_1} &\left(a_{12}(-\tau_{k,l}) \right. \\ &\left. + a_{12}(M_1 - \tau_{k,l}) + a_{12}(-M_1 - \tau_{k,l})\right) \end{aligned}$$

where $\tau_{k,l} = M_1(\frac{k}{M_1} - \frac{l}{M_2})$.

b) If φ_1 and φ_2 have the same parity, then the correlation is expressed as

$$[\mathbf{A}_{12}]_{k,l} = \frac{1}{M_1} \left(a_{12}(|\tau_{k,l}|) + a_{12}(|\tau_{k,l}| - M_1)\right)$$

with $\tau_{k,l} = M_1(\frac{k}{M_1} - \frac{l}{M_2})$.

Observe that, if $M_1 = M_2$, further simplifications of Proposition 1 are obtained. For instance, the case when $\varphi_1 = \varphi_2$ or $\varphi_2 = \dot{\varphi}_1 = \frac{\mathrm{d}\varphi_1}{\mathrm{d}t}$ implies that $a_{12} = \dot{a}_{11}$. Also note that, due to the periodicity of the generators and to $M_1 = M_2$, the matrix $\mathbf{A}_{12}$ is circulant and thus entirely specified by its M_1 entries $\{[\mathbf{A}_{12}]_{0,l}\}_{l\in[0\ldots M_1-1]}$ [25]. This matrix is diagonalizable, and hence, an explicit expression for its inverse is easy to obtain.

B. Specific Cases of a_{12} in Practice

B-splines are basis functions that are widely used in signal processing and have interesting mathematical properties that can be exploited to simplify the proposed inner-product calculus. In this section, we illustrate how the expression of a_{12} is simplified for specific cases that frequently appear in practice and that involve B-splines.

1) B-Splines Revisited: (Exponential) B-splines are popular not only in sampling and approximation theory but also to represent parametric curves and surfaces. They are compactly supported and have optimal approximation and reproduction properties [26]. An exponential B-spline of order n is fully characterized by its unordered list of (complex valued) poles $\boldsymbol{\alpha} = (\alpha_1, \alpha_2, \ldots, \alpha_n)$. It is supported in $[0, n]$ and its causal form is characterized in the frequency domain as $\hat{\beta}_{\boldsymbol{\alpha}}(\omega) = \prod_{p=1}^{n} \frac{1 - e^{\alpha_p - j\omega}}{j\omega - \alpha_p}$. If all the poles are equal to zero (i.e., $\boldsymbol{\alpha} = \mathbf{0}_n$), we obtain the classical polynomial B-splines of degree $(n-1)$. A function $\varphi \propto \beta_{\boldsymbol{\alpha}}$ that satisfies the partition-of-unity condition can only be constructed if the exponential B-spline $\beta_{\boldsymbol{\alpha}}$ contains at least one vanishing pole (i.e., if 0 is an element

of $\boldsymbol{\alpha}$). The notation $\boldsymbol{\alpha}_1 \cup \boldsymbol{\alpha}_2$ describes the union of two lists of poles $\boldsymbol{\alpha}_1$ and $\boldsymbol{\alpha}_2$. The notation $\boldsymbol{\alpha} \setminus \{\alpha_p\}$ describes a list from which the element α_p has been excluded.

2) Correlation Between Polynomial B-Splines: The function a_{12} for the case of polynomial B-splines of different orders is determined according to Proposition 2.

Proposition 2: Let $\varphi_1 = \beta_{\mathbf{0}_n}$ and $\varphi_2 = \beta_{\mathbf{0}_m}$. Then

$$a_{12}(t) = \left(\frac{M_2}{M_1}\right)^{m-1} \sum_{l=0}^{n} \sum_{k=0}^{m} \binom{n}{l} \binom{m}{k} (-1)^{l+k+m} \times \varsigma^{n+m-1}\left(t + \frac{kM_1}{M_2} - l\right)$$

where ς^n is the *polynomial simple element* of degree n defined as $\varsigma^n(t) = \frac{t^n \mathrm{sgn}(t)}{2(n!)}$ for $n \in \mathbb{N}$.
The proof is given in Appendix B.

3) Correlation Between Exponential B-Splines: In the case where $\varphi_1 = \beta_{\boldsymbol{\alpha}_1}$ and $\varphi_2 = \beta_{\boldsymbol{\alpha}_2}$ are two exponential B-splines of order n_1 and n_2, respectively, and $M_1 = M_2$, we obtain

$$a_{12}(t) = \left(\prod_{n=1}^{n_2} e^{\alpha^*_{2,n}}\right) \beta_{\boldsymbol{\alpha}_1 \cup (-\boldsymbol{\alpha}_2^*)}(t + n_2) \tag{9}$$

where $\boldsymbol{\alpha}^*$ is the complex conjugate of $\boldsymbol{\alpha}$ [26]. Equation (9) corresponds to the cross-correlation of two exponential B-splines which yields an exponential B-spline of augmented order. Proposition 3 provides a simplified expression of (9) in the case where $\varphi_1 = \beta_{\boldsymbol{\alpha}}$ and $\varphi_2 = \dot{\varphi}_1$.

Proposition 3: Let $\varphi_1 = \beta_{\boldsymbol{\alpha}}$ be an exponential B-spline of order n that contains at least one vanishing pole (we suppose $\alpha_n = 0$), and $\varphi_2 = \dot{\beta}_{\boldsymbol{\alpha}}$. Then

$$a_{12}(t) = -\left(\prod_{l=1}^{n-1} e^{\alpha_l^*}\right) \Delta\beta_{\boldsymbol{\alpha} \cup (-(\boldsymbol{\alpha}^* \setminus \{0\}))}(t + n - 1)$$

where $\Delta f(t) = (f(t) - f(t-1))$ denotes the finite difference of f.
The proof is given in Appendix C. Note that, the same kind of formula also applies for fractional B-splines [27].

III. Applications

A. Resampling of a Spline Curve

The general scheme to reduce the size of a polygonal or spline curve $\boldsymbol{r}_1$ is to decrease its number M_1 of control points [28]. The standard method is to simply resample the curve [11]. However, this does not take into account details localized between two samples, which alters the accuracy of the approximation while eventually introducing aliasing artifacts [29]. We propose a new method which consists in computing the L_2 approximation $\boldsymbol{r}_2$ of the curve $\boldsymbol{r}_1$, with $M_1 > M_2$. This is equivalent to compute $\arg\min_{\mathbf{C}_2} \|\boldsymbol{r}_1 - \boldsymbol{r}_2\|^2_{L_2}$. It is not difficult to show that the general solution, in the context of our framework, is given by

$$\mathbf{C}_2 = \mathbf{A}_{22}^{-1} \mathbf{A}_{21} \mathbf{C}_1 \tag{10}$$

where $\mathbf{C}_1$ and $\mathbf{C}_2$ are the coefficient matrices of size $(M_1 \times 2)$ and $(M_2 \times 2)$, respectively. The entries of the matrices $\mathbf{A}_{21}$ and $\mathbf{A}_{22}$, of size $(M_2 \times M_1)$ and $(M_2 \times M_2)$, respectively, can be evaluated using Proposition 1 and Proposition 2.

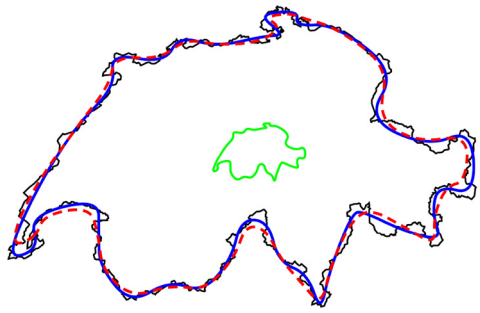

Fig. 1. Resampling of the outline (black curve) of the map of Switzerland. Solid blue curve and dashed red curve: resampled versions obtained by the L_2 approximation and sampling methods, respectively, with $M_2 = 40$ samples. Green curve: reduced version of the map obtain with the L_2 approximation.

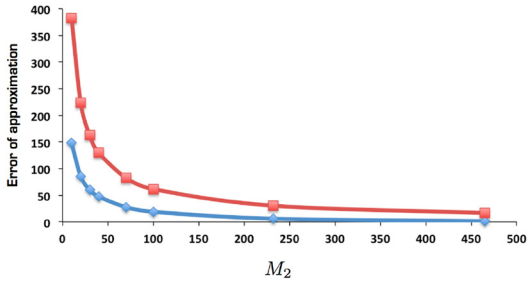

Fig. 2. Comparison of the approximation error for the L_2 approximation method (blue diamonds) and the sampling method (red squares).

To experimentally compare resampling and approximation, we propose to reduce the outline $\boldsymbol{r}_1$ of the map of Switzerland defined by $M_1 = 930$ control points interpolated with the linear spline $\varphi_1 = \beta_{(0,0)}$ (Fig. 1, black curve). We resample $\boldsymbol{r}_1$ with both the sampling and the L_2 approximation methods for different values of $M_2 < M_1$ control points and in the basis of the quadratic spline $\varphi_2 = \beta_{(0,0,0)}$. We illustrate the case $M_2 = 40$ in Fig. 1. We observe that the resampled curves act as smoothed versions of $\boldsymbol{r}_1$ with less details and increased regularity. We compute their approximation error for each value of M_2. In Fig. 2, it is seen that the best approximation of the reduced version of the map, without aliasing artifacts, is obtained with our proposed method (Fig. 1, green curve).

B. Area Enclosed by a Parametric Curve

In this section, we consider a non-intersecting curve $\boldsymbol{r}_1$ and its derivative $\dot{\boldsymbol{r}}_1 = M_1 \mathbf{C}_1^\mathsf{T} \dot{\boldsymbol{\varphi}}_1$. The factor M_1 is due to the normalization in (4). The computation of the area enclosed by a parametric curve usually involves the evaluation of a surface integral. We propose instead to use Green's theorem [15] to express this surface integral as a contour integral, which results in a signed area expressed as

$$I = \oint_{\boldsymbol{r}_1} f_{y_1} \mathrm{d} f_{x_1} = \langle f_{y_1}, \dot{f}_{x_1} \rangle_{L_2([0,1])} = M_1 \mathbf{c}_{y_1}^\mathsf{T} \mathbf{A}_{12} \mathbf{c}_{x_1} \tag{11}$$

where $\varphi_2 = \dot{\varphi}_1$, $M_2 = M_1$, and $\mathbf{c}_{x_1}$ and $\mathbf{c}_{y_1}$ are the first and second columns of the matrix (7), respectively. The sign of I depends on the direction in which the curve is traversed.

In the case of centered (exponential) B-splines, (11) is easily computed. For $\varphi_1 = \beta_{\boldsymbol{\alpha}}$, we evaluate the entries of the matrix $\mathbf{A}_{12}$ using Corollary 1a) and Proposition 3. We obtain

$$[\mathbf{A}_{12}]_{k,l} = \frac{1}{M_1} \sum_{n=-1}^{1} \Delta_c \beta_{\boldsymbol{\alpha} \cup (\boldsymbol{\alpha} \setminus \{0\})}(k - l + nM_1)$$

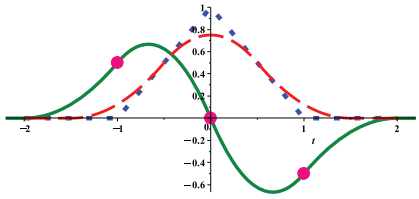

Fig. 3. Blue dots: centered linear B-spline; red dashes: centered quadratic B-spline; green line: $\Delta_c\beta_{(0,0,0)}$; pink circles: $\Delta_c\beta_{(0,0,0)}(k)$ for $k=-1,0,1$.

where $\Delta_c f(t)=(f(t+\frac{1}{2})-f(t-\frac{1}{2}))$ denotes the centered finite difference of f. As the matrix is circulant, we only compute these values for $k=0$ and $l\in[0\dots M_1-1]$. For instance, if the parametric curve (6) is constructed with the centered linear B-spline $\varphi_1=\beta_{(0,0)}$ (Fig. 3, dotted blue curve), we have $\Delta_c\beta_{\boldsymbol{\alpha}\cup(\boldsymbol{\alpha}\setminus\{0\})}=\Delta_c\beta_{(0,0,0)}$ (Fig. 3, green curve), where $\beta_{(0,0,0)}$ is the centered quadratic B-spline (Fig. 3, dashed red curve). Then, each row of the correlation matrix is expressed as a periodic shift of the centered finite difference $\left[\frac{1}{2}\ \ 0\ \ -\frac{1}{2}\right]$.

IV. Conclusion

The computation of inner products between periodized basis functions requires the evaluation of a correlation matrix $\mathbf{A}_{12}$. This matrix frequently appears in periodic settings in classical L_2-based signal processing as well as in image processing when dealing with closed parametric curves. We have presented exact formulas to evaluate its entries and gave simplified expressions for particular cases. As the correlation matrix itself does not depend on the weights (or control points) that specify the signal (or parametric curve), its values can be precomputed and stored in lookup tables for a fast evaluation of L_2 distances. We also proposed an L_2 approximation method to resample a curve, which consists in describing the curve in a different basis using less control points. These new points are found by a least-squares minimization: the general solution requires the evaluation of two correlation matrices that can be precomputed using our proposed formulas. We compared our approach to the classical uniform resampling method and showed that the best approximation was obtained with our method. We also illustrated the use of the proposed formulas to evaluate the area enclosed by a parametric curve. Our inner-product calculus allows for a fast and exact evaluation of correlation integrals which frequently appear in practice and are often only approximately computed up to date.

Appendix

A. Proof of Proposition 1

$$\begin{aligned}
&\int_0^1 \varphi_{1,\mathrm{per}}(M_1t-k)\varphi_{2,\mathrm{per}}(M_2t-l)\mathrm{d}t\\
&=\int_{-\frac{l}{M_2}}^{1-\frac{l}{M_2}}\varphi_{1,\mathrm{per}}\left(M_1\left(t'+\frac{l}{M_2}\right)-k\right)\varphi_{2,\mathrm{per}}(M_2t')\mathrm{d}t'\\
&=\int_{\frac{a_2}{M_2}}^{1+\frac{a_2}{M_2}}\varphi_{1,\mathrm{per}}\left(M_1\left(t+\frac{l}{M_2}\right)-k\right)\varphi_2(M_2t)\mathrm{d}t\\
&=\int_{\frac{a_2}{M_2}}^{1+\frac{a_2}{M_2}}\sum_{m=-\infty}^{+\infty}\varphi_1\Bigg(M_1t-\underbrace{M_1\left(m+\frac{k}{M_1}-\frac{l}{M_2}\right)}_{\tau_{k,l,m}}\Bigg)\varphi_2(M_2t)\mathrm{d}t.
\end{aligned}\tag{12}$$

We set $m_1=\lceil\min(p_1,p_2)\rceil$, $m_2=1+\lfloor\max(p_1,p_2)\rfloor$, $p_1=(\frac{1}{M_2}(a_2+l)-\frac{1}{M_1}(a_1+k))$, and $p_2=(\frac{1}{M_2}(a_2+l)-\frac{1}{M_1}(b_1+k))$. Now, (12) is simplified as

$$\begin{aligned}
&\sum_{m=m_1}^{m_2}\int_{\frac{a_2}{M_2}}^{1+\frac{a_2}{M_2}}\varphi_1(M_1t-\tau_{k,l,m})\varphi_2(M_2t)\mathrm{d}t\\
&=\frac{1}{M_1}\sum_{m=m_1}^{m_2}\int_{\mathbb{R}}\varphi_1(t-\tau_{k,l,m})\varphi_2\left(\frac{M_2}{M_1}t\right)\mathrm{d}t\\
&=\frac{1}{M_1}\sum_{m=m_1}^{m_2}\int_{\mathbb{R}}\varphi_1(t)\varphi_2\left(\frac{M_2}{M_1}(t+\tau_{k,l,m})\right)\mathrm{d}t\\
&=\frac{1}{M_1}\sum_{m=m_1}^{m_2}a_{12}(-\tau_{k,l,m})
\end{aligned}$$

where $a_{12}(t)=(\varphi_1*\varphi_2(-\frac{M_2}{M_1}\cdot))(t)$ and we have used the fact that $\varphi_2(\pm\frac{M_2}{2}-M_2n)=0$ if $|n|\geq\frac{\mathrm{supp}\{\varphi_2\}+M_2}{2M_2}$ and that $\varphi_1(\pm\frac{M_1}{2}-M_1p)=0$ if $|p|\geq\frac{\mathrm{supp}\{\varphi_1\}+M_1}{2M_1}$. ■

B. Proof of Proposition 2

We define by Δ_b^n the nth-order causal finite-difference operator with $b\neq0$, defined as $\Delta_b^nf(t)=\sum_{k=0}^n\binom{n}{k}(-1)^kf(t-\frac{k}{b})$. The Fourier transform $\mathcal{F}$ of the causal polynomial B-spline $\beta_{\mathbf{0}_n}$ is given by

$$\begin{aligned}
\mathcal{F}\{\beta_{\mathbf{0}_n}(t)\}(\omega)=\hat\beta_{\mathbf{0}_n}(\omega)&=\left(\frac{1-e^{-j\omega}}{j\omega}\right)^n\\
&=\hat\Delta_1^n(\omega)\mathcal{F}\{\varsigma^{n-1}(t)\}(\omega)
\end{aligned}$$

where $\mathcal{F}\{\varsigma^n(t)\}(\omega)=\frac{1}{(j\omega)^{n+1}}$. Let $\varphi_1=\beta_{\mathbf{0}_n}$ and $\varphi_2=\beta_{\mathbf{0}_m}$. We compute

$$\begin{aligned}
a_{12}(t)&=\left(\beta_{\mathbf{0}_n}*\beta_{\mathbf{0}_m}\left(-\frac{M_2}{M_1}\cdot\right)\right)(t)\\
&=\mathcal{F}^{-1}\left\{\hat\beta_{\mathbf{0}_n}(\omega)\frac{M_1}{M_2}\hat\beta_{\mathbf{0}_m}\left(-\frac{M_1}{M_2}\omega\right)\right\}(t)\\
&=\mathcal{F}^{-1}\left\{\left(\frac{1-e^{-j\omega}}{j\omega}\right)^n\frac{M_1}{M_2}\left(\frac{1-e^{j\frac{M_1}{M_2}\omega}}{-j\frac{M_1}{M_2}\omega}\right)^m\right\}(t)\\
&=\mathcal{F}^{-1}\left\{(-1)^m\left(\frac{M_2}{M_1}\right)^{m-1}\frac{(1-e^{-j\omega})^n(1-e^{j\frac{M_1}{M_2}\omega})^m}{(j\omega)^{n+m}}\right\}(t)\\
&=(-1)^m\left(\frac{M_2}{M_1}\right)^{m-1}\mathcal{F}^{-1}\left\{\hat\Delta_1^n(\omega)\hat\Delta_{-\frac{M_2}{M_1}}^m(\omega)\hat\varsigma^{n+m-1}(\omega)\right\}(t)\\
&=\left(\frac{M_2}{M_1}\right)^{m-1}\sum_{l=0}^n\sum_{k=0}^m\binom{n}{l}\binom{m}{k}(-1)^{l+k+m}\\
&\quad\times\varsigma^{n+m-1}\left(t+\frac{kM_1}{M_2}-l\right).
\end{aligned}$$ ■

C. Proof of Proposition 3

The derivative of an exponential B-spline that contains a vanishing pole is given by $\dot\beta_{\boldsymbol{\alpha}\cup\{0\}}=\Delta\beta_{\boldsymbol{\alpha}}$. Let $\varphi_1=\beta_{\boldsymbol{\alpha}}$ and $\varphi_2=\dot\varphi_1$. Using (9), we compute

$$\begin{aligned}
a_{12}(t)&=(\beta_{\boldsymbol{\alpha}}*\dot\beta_{\boldsymbol{\alpha}}(-\cdot))(t)\\
&=-(\beta_{\boldsymbol{\alpha}}*\Delta\beta_{\boldsymbol{\alpha}\setminus\{0\}}(-\cdot))(t)\\
&=-\left(\prod_{l=1}^{n-1}e^{\alpha_l^*}\right)\Delta\beta_{\boldsymbol{\alpha}\cup(-(\boldsymbol{\alpha}^*\setminus\{0\}))}(t+n-1).
\end{aligned}$$ ■

REFERENCES

[1] P. Dragotti, M. Vetterli, and T. Blu, "Sampling moments and reconstructing signals of finite rate of innovation: Shannon meets Strang-Fix," *IEEE Trans. Signal Process.*, vol. 55, no. 5, pp. 1741–1757, May 2007.

[2] I. Selesnick, "Interpolating multiwavelet bases and the sampling theorem," *IEEE Trans. Signal Process.*, vol. 47, no. 6, pp. 1615–1621, Jun. 1999.

[3] J. Berent, P. Dragotti, and T. Blu, "Sampling piecewise sinusoidal signals with finite rate of innovation methods," *IEEE Trans. Signal Process.*, vol. 58, no. 2, pp. 613–625, Feb. 2010.

[4] M. Vetterli, "Wavelets, approximation, and compression," *IEEE Signal Process. Mag.*, vol. 18, no. 5, pp. 59–73, Sep. 2001.

[5] N. Leonardi and D. Van De Ville, "Tight wavelet frames on multislice graphs," *IEEE Trans. Signal Process.*, vol. 61, no. 13, pp. 3357–3367, Jul. 2013.

[6] S. Mallat, "A theory for multiresolution signal decomposition: The wavelet representation," *IEEE Trans. Pattern Anal. Mach. Intell.*, vol. 11, no. 7, pp. 674–693, Jul. 1989.

[7] A. N. Akansu, W. A. Serdijn, and I. W. Selesnick, "Emerging applications of wavelets: A review," *Phys. Commun.*, vol. 3, no. 1, pp. 1–18, Mar. 2010.

[8] I. Selesnick, R. Baraniuk, and N. Kingsbury, "The dual-tree complex wavelet transform," *IEEE Signal Process. Mag.*, vol. 22, no. 6, pp. 123–151, Nov. 2005.

[9] I. Daubechies, *Ten Lectures on Wavelets*. Philadelphia, PA, USA: Society for Industrial and Applied Mathematics, 1992.

[10] A. Aldroubi and H. Feichtinger, "Exact iterative reconstruction algorithm for multivariate irregularly sampled functions in spline-like spaces: The l_p-theory," *Proc. Amer. Math. Soc.*, vol. 126, no. 9, pp. pp. 2677–2686, Sep. 1998.

[11] M. Unser, "Sampling—50 Years after Shannon," *Proc. IEEE*, vol. 88, no. 4, pp. 569–587, Apr. 2000.

[12] F. M. Candocia and J. C. Príncipe, "Comments on 'Sinc interpolation of discrete periodic signals,'" *IEEE Trans. Signal Process.*, vol. 46, no. 7, pp. 2044–2047, Jul. 1998.

[13] Y. Lee, J. Cheatham, and J. Wiesner, "Application of correlation analysis to the detection of periodic signals in noise," *Proc. IRE*, vol. 38, no. 10, pp. 1165–1171, Oct. 1950.

[14] S. Qian and D. Chen, "Joint time-frequency analysis," *IEEE Signal Process. Mag.*, vol. 16, no. 2, pp. 52–67, Mar. 1999.

[15] M. Jacob, T. Blu, and M. Unser, "An exact method for computing the area moments of wavelet and spline curves," *IEEE Trans. Pattern Anal. Mach. Intell.*, vol. 23, no. 6, pp. 633–642, Jun. 2001.

[16] M. Kass, A. Witkin, and D. Terzopoulos, "Snakes: Active contour models," *Int. J. Comput. Vis.*, vol. 1, no. 4, pp. 321–331, Jan. 1987.

[17] X. Bresson, S. Esedoglu, P. Vandergheynst, J.-P. Thiran, and S. Osher, "Fast global minimization of the active contour/snake model," *J. Math. Imag. Vis.*, vol. 28, no. 2, pp. 151–167, 2007.

[18] J. K. Mogali, A. K. Pediredla, and C. S. Seelamantula, "Template-based active contours," *CoRR*, vol. abs/1312.0760, 2013. [Online]. Available: http://arxiv.org/abs/1312.0760

[19] R. Delgado-Gonzalo, V. Uhlmann, D. Schmitter, and M. Unser, "Snakes on a plane," *IEEE Signal Process. Mag.*, vol. 32, no. 1, pp. 41–48, Jan. 2015.

[20] D. Schmitter, R. Delgado-Gonzalo, G. Krueger, and M. Unser, "Atlas-free brain segmentation in 3D proton-density-like MRI images," in *Proc 11th IEEE Int. Symp. Biomed. Imag.: Nano Macro (ISBI'14)*, Beijing, China, Apr. 29–May 2, 2014, pp. 629–632.

[21] D. Schmitter, R. Delgado-Gonzalo, and M. Unser, "Trigonometric interpolation kernel to construct deformable shapes for user-interactive applications," *IEEE Signal Process. Lett.*, vol. 22, no. 11, pp. 2097–2101, Nov. 2015.

[22] D. Schmitter, R. Delgado-Gonzalo, and M. Unser, "A family of smooth and interpolatory basis functions for parametric curve and surface representation," *Appl. Math. Comput.*, vol. 272, no. 1, pp. 53–63, Jan. 2016.

[23] L. Rebollo-Neira and D. Lowe, "Optimized orthogonal matching pursuit approach," *IEEE Signal Process. Lett.*, vol. 9, no. 4, pp. 137–140, Apr. 2002.

[24] S. Mallat, *A Wavelet Tour of Signal Processing*. New York, NY, USA: Academic, 1999.

[25] P. Davis, *Circulant Matrices*. Hoboken, NJ, USA: Wiley, 1979.

[26] M. Unser and T. Blu, "Cardinal exponential splines: Part I—Theory and filtering algorithms," *IEEE Trans. Signal Process.*, vol. 53, no. 4, pp. 1425–1438, Apr. 2005.

[27] M. Unser and T. Blu, "Fractional splines and wavelets," *SIAM Rev.*, vol. 42, no. 1, pp. 43–67, Mar. 2000.

[28] J. A. Parker, R. V. Kenyon, and D. E. Troxel, "Comparison of interpolating methods for image resampling," *IEEE Trans. Med. Imag.*, vol. 2, no. 1, pp. 31–39, Mar. 1983.

[29] M. Jacob, T. Blu, and M. Unser, "Sampling of periodic signals: A quantitative error analysis," *IEEE Trans. Signal Process.*, vol. 50, no. 5, pp. 1153–1159, May 2002.